# Title: Rapid and Stimulus-Specific Deviance Detection in the Human Inferior Colliculus

Abbreviated title: Subcortical Auditory Deviance Detection in Humans

Authors: Johannes Wetekam[1,*], Nell Gotta[1], Luciana López-Jury[2], Julio Hechavarría[1,3,×,*], Manfred Kössl[1,×]

1. Department of Neurobiology and Biological Sensors
   Institute of Cell Biology and Neuroscience, Goethe University
   Max-von-Laue-Str. 13, 60438 Frankfurt am Main, Germany
2. Max Planck Institute for Brain Research
   Max-von-Laue-Str. 4, 60438 Frankfurt am Main, Germany
3. Ernst Strüngmann Institute (ESI) for Neuroscience
   Deutschordenstraße 46, 60528 Frankfurt am Main, Germany

×Shared last authorship

*Corresponding authors: Johannes Wetekam: johannes.p.wetekam@esi-frankfurt.de, Julio Hechavarría: julio.hechavarria@esi-frankfurt.de

Number of pages: 30, Number of figures: 4, Number of words Abstract: 235, Number of words Introduction: 596, Number of words Results: 980, Number of words Discussion: 1548

Acknowledgements

This work was funded by the Deutsche Forschungsgemeinschaft [KO 987/14-1].

Conflict of Interest

The authors declare no competing interests.

## Abstract

Auditory deviance detection, the neural process by which unexpected stimuli are identified within repetitive acoustic environments, is crucial for survival. While this phenomenon has been extensively studied in the cortex, recent evidence indicates that it also occurs in subcortical regions, including the inferior colliculus (IC). However, compared to animal studies, research on subcortical deviance detection in humans is often constrained by methodological limitations, leaving several important questions unanswered. This study aims to overcome some of these limitations by employing auditory brainstem responses (ABRs) to investigate the earliest neural correlates of deviance detection in humans, with a focus on the IC. We presented healthy participants with low- and high-frequency chirps in an oddball paradigm and observed significant deviance detection effects in the ABR, specifically when low-frequency chirps were used as deviants within a context of high-frequency standards. These effects manifested as larger and faster ABRs to deviant stimuli, with the strongest responses occurring at higher stimulation rates. Our findings suggest that the human IC exhibits rapid, stimulus-specific deviance detection with differential modulation of response amplitude and latency. The data indicate that the temporal dynamics of novelty detection in humans align well with the data reported in animals, helping to bridge the gap between animal and human research. By uncovering previously unknown characteristics of subcortical deviance detection in humans, this study highlights the value of ABR recordings with excellent temporal resolution in investigating subcortical deviance detection processes.



**Keywords**: stimulus-specific adaptation, mismatch negativity, auditory brainstem responses, predictive coding, repetition suppression, brainstem

## 1. Introduction

The ability of the brain to detect unexpected acoustic stimuli in an otherwise repetitive environment is known as auditory deviance detection and has been the focus of extensive research over the last decades. Through a combination of animal and human studies, researchers have characterised this phenomenon with remarkable detail, providing the foundation for our current understanding of deviance detection (Escera and Malmierca, 2014; Carbajal and Malmierca, 2018). Initially thought to be limited to the cortex (Näätänen et al., 1978; Ulanovsky et al., 2003, 2004), pioneering studies in rodents revealed that deviance detection is ubiquitous throughout the brain, with evidence found in several subcortical regions (Kraus et al., 1994a, 1994b; Pérez-González et al., 2005; Malmierca et al., 2009; Antunes et al., 2010; Zhao et al., 2011; Patel et al., 2012). Building on these findings, subsequent research demonstrated that correlates of deviance detection can also be observed in the subcortical auditory system of humans (Chandrasekaran et al., 2009; Skoe and Kraus, 2010; Slabu et al., 2012; Cacciaglia et al., 2015; Tabas et al., 2020; Tabas and Kriegstein, 2024), supporting the idea of a widespread novelty detection mechanism within the mammalian brain (Escera et al., 2014; Parras et al., 2017; Tabas and von Kriegstein, 2021).

Nevertheless, while findings from animal and human studies often align and complement each other, methodological limitations in human research sometimes hinder precise correlations between the two research lines. Most research on deviance detection in animals relies on invasive electrophysiological recordings, which provide high temporal and spatial resolution (Nelken, 2014). In contrast, human studies primarily utilise non-invasive techniques such as electroencephalography (EEG), magnetoencephalography (MEG), functional magnetic resonance imaging (fMRI) and the frequency-following response (FFR), each with its own limitations. EEG and MEG offer excellent temporal and spatial resolution, respectively, but are largely limited to detecting superficial neural activity and thus mainly reflect cortical

processing. fMRI can capture activity from deeper brain structures but suffers from significantly lower temporal resolution. The FFR represents a sustained compound response of cortical and subcortical sources (Coffey et al., 2016, 2019), making it challenging to attribute observed effects to specific auditory nuclei. As a result, our current understanding of subcortical deviance detection in humans remains limited, at least when compared with cortical deviance detection in humans, which has been extensively investigated, particularly in the form of mismatch negativity (MMN) (Näätänen et al., 2007; Winkler, 2007; Fitzgerald and Todd, 2020) .

The aim of this study is to quantify the dynamics of human subcortical deviance detection, with a focus on IC activity. To achieve this, we measured auditory brainstem responses (ABRs) to low- and high-frequency chirp stimuli (Fig. 1a) that were designed to maximise ABR amplitude while ensuring a clear frequency difference between the deviant and standard stimuli in an oddball paradigm (Fig. 1b). ABRs are non-invasively recorded population responses that enabled us to overcome many of the limitations described in the preceding text. They have been successfully used to study subcortical deviance detection in animals (Duque et al., 2018; Wetekam et al., 2022, 2024) and offer several advantages for the specific aims of this study. ABRs are evoked electrical responses that are generated solely in the brainstem, thus excluding any potential cortical contributions to the signal. Furthermore, the high temporal resolution of ABRs, compared to fMRI recordings, enabled us to analyse changes not only in response amplitude but also in peak latency. The good temporal resolution also allowed us to examine the effects of subcortical deviance detection over time on a trial-by-trial basis, offering novel insights into human subcortical deviance detection and narrowing the gap between human and animal research.

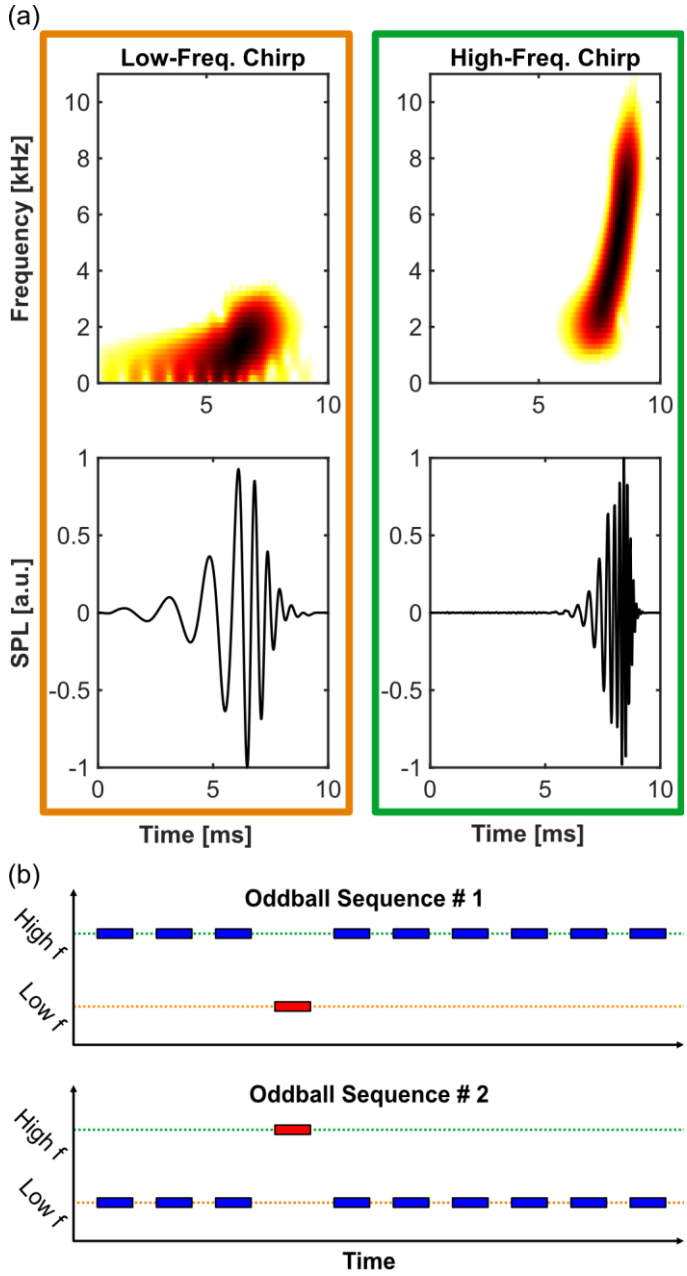


*Figure 1: Used stimuli and stimulation protocol. (a) Spectrograms (top) and oscillograms (bottom) of a low-frequency chirp (orange frame) and a high-frequency chirp (green frame) that were used as stimuli in this study. (b) Schematic representation of the oddball paradigm; blue: high-probability standard, red: low-probability deviant.*

## 2. Material and Methods

**Participants**

ABRs of 27 participants (8 males, 19 females), aged between 20 and 40 years (mean age = 25.5 years) and with normal hearing, were recorded for the current study. Informed consent was obtained from each participant prior to recording, and all subjects received monetary compensation for their participation. The study was approved by the Goethe University Frankfurt Ethics Committee (reference number: E 27/23) and was conducted in accordance with the WMA Declaration of Helsinki. Before the recording began, a two-alternative forced choice test was used to determine each participant's individual hearing thresholds for the stimuli used during the ABR recording.

**Stimulation and recording procedure**

Two artificially generated chirps, differing in their frequency composition, were used as stimuli (Fig. 1a). These chirps were designed to maximise ABR amplitudes by compensating for the cochlear traveling wave delay, as described by Fobel and Dau (2004), Elberling et al. (2007) and Elberling and Don (2008). The chirp design was based on the latency-frequency function derived from narrowband ABR data by Don et al. (2005). These chirp stimuli effectively evoked a prominent IC-generated wave V (Buchwald and Huang, 1975; Henry, 1979; Caird and Klinke, 1987; Land et al., 2016), thereby maximising the overall ABR amplitude. However, the earlier ABR components (waves I-IV) were typically less pronounced compared to those evoked by click stimuli. The stimuli were created with a logarithmic frequency distribution: the low-frequency chirp ranged from 500 Hz to 2 kHz, and the high-frequency chirp ranged from 2 kHz to 8 kHz. Importantly, although both chirps had different durations (low-frequency chirp: 9 ms, high-frequency chirp: 4 ms), their design ensured a simultaneous activation of the entire basilar membrane, occurring temporally close to the peak of each stimulus. This characteristic, coupled with the fact that ABRs reflect onset

responses, makes the difference in stimulus duration irrelevant in the context of this study. The signals were digitally generated using custom-written Matlab (MathWorks) scripts, converted from digital to analogue by a 192 kHz Fireface UC soundcard (RME Audio), and delivered to the participant's right ear via an ER-3C earphone (10 Ω, Etymotic Research).

During the ABR recording, stimuli were presented to the participants at 40 dB HL, in two pseudo-randomly arranged oddball sequences. In the first sequence, the high-frequency chirp was presented as high-probability standard (90 %, 9000 repetitions), while the low-frequency chirp was presented as low-probability deviant (10 %, 1000 repetitions). The sequence was then repeated with the roles of the deviant and standard stimuli swapped (Fig. 1b), resulting in two distinct responses for each stimulus: one when perceived as the standard and one as the deviant. The recordings were conducted at three different stimulus presentation rates: 40 Hz, 33 Hz and 20 Hz.

ABRs were recorded using two Ag-AgCl electrodes placed on the participant’s skin: one at the vertex (Cz, active) and the other on the ipsilateral earlobe (reference). A third electrode on the forehead served as the ground. Impedance was reduced to less than 10 kΩ, and data was collected at a sampling rate of 10 kHz. The recordings were conducted in an electrically and sound-insulated booth, where participants sat comfortably in a reclining chair. They were instructed to relax, keep their eyes closed, and minimise movement during the recording.

**Data processing and statistical evaluation**

All data analysis and statistical evaluation were conducted using Matlab. The recorded data was bandpass filtered using a 70-1500 Hz Butterworth filter (4th order). For baseline correction, the mean response amplitude of each trial was calculated within a 5 ms time window immediately before ABR onset. Due to the relatively long and unequal rise times of the low- and high-frequency chirps (6.5 ms and 3 ms, respectively) (Fig. 1), the end of the baseline correction window was aligned with the time point of maximal stimulus amplitude,

corresponding to the time point of basilar membrane activation. The mean amplitude value within this window was then subtracted from the entire trial, resulting in a mean pre-ABR activity of 0 µV.

For averaging, only standard trials followed by a deviant trial were considered, and only deviants preceded by a standard were included in the analysis. This approach ensured that the same number of deviant and standard trials were used to calculate the average response for each participant (ranging between 851 and 914 trials) in order to maintain equal variance across conditions. All trials were corrected for the sound travel delay caused by the distance between the speaker and the ear (26 cm). In each time-voltage graph, the x-axis value of 0 ms represents the time point when the maximal stimulus amplitude reached the ear.

To identify differences between deviant and standard ABRs, a cluster-based permutation analysis was performed (in accordance to Candia-Rivera and Valenza, 2022). First, a Wilcoxon rank-sum test was used to compare the deviant and standard ABRs at each time point. If more than five consecutive time points had p-values below 0.01, these points were grouped into a cluster. Next, the z-values for each time point within a cluster were summed to obtain the cluster weight. To determine whether these observed clusters were significant, a permutation distribution was generated. Deviant and standard trials were randomly shuffled, and the average ABR waveforms were recalculated, producing two new shuffled responses for each subject. Clusters and their weights were then recomputed. This permutation procedure was repeated 1000 times, creating a distribution of cluster weights under the null hypothesis that no real difference exists between deviant and standard responses. The observed cluster weights were then compared to this permutation distribution. A cluster was considered statistically significant if its weight exceeded 95 % of the values in the permutation distribution, corresponding to a p-value of 0.05. The p-values of all observed

clusters were corrected for multiple comparisons using the Benjamini-Hochberg false discovery rate (FDR) method (Benjamini and Hochberg, 1995).

Given that significant clusters were only found when the low-frequency chirp was used as the target stimulus, all subsequent analyses focused solely on responses to the low-frequency chirp. To determine whether the significant differences between the waveforms of deviant and standard ABRs were due to variations in ABR peak-to-peak amplitude and peak V latency, additional statistical tests were conducted. These parameters were calculated within predefined analysis windows. The peak-to-peak amplitude was measured within a window comprising all significant clusters, as identified by the cluster-based permutation analysis (2.7-9.2 ms post-stimulus peak). For peak V latency, a later window onset was selected (5-9.2 ms post-stimulus peak) to focus exclusively on wave V and minimise data variability. Both peak-to-peak amplitude and peak V latency were confirmed to be normally distributed using Lilliefors tests.

To assess the effects of stimulus probability (deviant, standard) and stimulus repetition rate (40 Hz, 33 Hz, 20 Hz) on ABR peak-to-peak amplitude and peak V latency, a two-way analysis of variance (ANOVA) was performed, considering potential interactions between the two factors. In case of significant ANOVA results, post hoc t-tests were carried out, with adjustments for multiple comparisons using the Benjamini-Hochberg FDR method. Additionally, Cohen's *d* was calculated for each significant comparison to provide a measure of effect size (Cohen, 1988).

The second part of this study explored how ABR amplitude and peak latency are modulated by deviance detection as the repetition number of the standard stimulus increases following a deviant (Fig. 3a). Sequences containing a deviant and at least three consecutive standard responses were extracted from the oddball recording, and the deviant as well as the first, second and third standard response were averaged per participant (with trial numbers ranging

between 683 and 723). The effects of stimulus role (deviant, standard 1, standard 2, standard 3) and repetition rate (40 Hz, 33 Hz, 20 Hz) on ABR peak-to-peak amplitude and peak V latency were assessed using a two-way ANOVA, accounting for potential interactions. When significant results were identified in the ANOVA, post-hoc t-test comparisons were performed with Benjamini-Hochberg FDR correction, and Cohen's *d* was calculated for significant t-test outcomes to quantify the effect size. The data and code used for this study are freely available on G-Node (DOI: 10.12751/g-node.ffr8gt).

# 3. Results

**Deviance detection modulates ABR amplitude and latency**

To investigate the effects of deviance detection in the brainstem, ABRs were recorded using a low- and a high-frequency chirp stimulus, presented in an oddball paradigm (Fig. 1b). Previous animal studies have demonstrated that subcortical deviance detection is sensitive to the rate at which stimuli are presented (Malmierca et al., 2009; Antunes et al., 2010; Zhao et al., 2011; Ayala and Malmierca, 2012; Patel et al., 2012). Consequently, three different stimulation rates were tested: 40 Hz, which is a commonly used rate in ABR research, and two slower rates of 33 Hz and 20 Hz, to assess whether potential effects of subcortical human deviance detection are influenced by the rate of stimulation. A cluster-based permutation analysis was performed to determine which ABR components differed significantly between deviant and standard responses. For the low-frequency chirp, a significant cluster was identified between 8 and 10 ms after basilar membrane activation across all stimulus repetition rates (40 Hz: $p = 0.029$; 33 Hz: $p = 0.020$; 20 Hz: $p = 0.031$) (Fig. 2a). Additionally, at the fastest repetition rate of 40 Hz, a second, earlier significant cluster was observed between approximately 2.5 and 4 ms ($p < 0.001$) (Fig. 2a, top). In contrast, no significant clusters were detected for the high-frequency chirp responses (Fig. 2b), indicating that stimulus probability significantly affected ABRs only when the low-frequency chirp was the target stimulus.

To identify the response parameters responsible for the significant clusters observed in the low-frequency responses, ABR peak-to-peak amplitude and ABR peak V latency were calculated and compared using two-way ANOVAs, with stimulus probability (deviant, standard) and stimulus repetition rate (40 Hz, 33 Hz, 20 Hz) as factors. The dependent variables were calculated within predefined time windows, indicated by the vertical dashed lines (Fig. 2a,b). The window for peak-to-peak calculation covered all significant clusters

(from dark grey line, 2.7 ms, to black line, 9.2 ms) and the latency window was set to only cover peak V (from light grey line, 5.0 ms to black line, 9.2 ms). For the low-frequency chirp, the ANOVA revealed a significant effect of stimulus probability on both ABR peak-to-peak amplitude ($p = 4.9*10^{-4}$) and peak V latency ($p = 2.1*10^{-6}$). Post hoc t-tests comparing deviant and standard responses demonstrated that peak-to-peak amplitude was significantly different at the two faster repetition rates of 40 Hz ($p = 0.010$) and 33 Hz ($p = 0.006$), with large effect sizes (Cohen's $d > 0.8$) (Fig. 2c). Peak V latency was significantly different across all three tested repetition rates (40 Hz: $p = 0.005$; 33 Hz: $p = 0.007$; 20 Hz: $p = 0.007$), with large effect sizes for the two faster rates (Cohen's $d > 0.8$) and medium effect size for the slower rate (Cohen's d between 0.5 and 0.8) (Fig. 2d). These findings suggest that the cluster-based differences between deviant and standard responses can be attributed to a combined effect of peak-to-peak amplitude and peak V latency at the faster repetition rates (40 Hz and 33 Hz), and to peak V latency alone at the slower repetition rate (20 Hz).

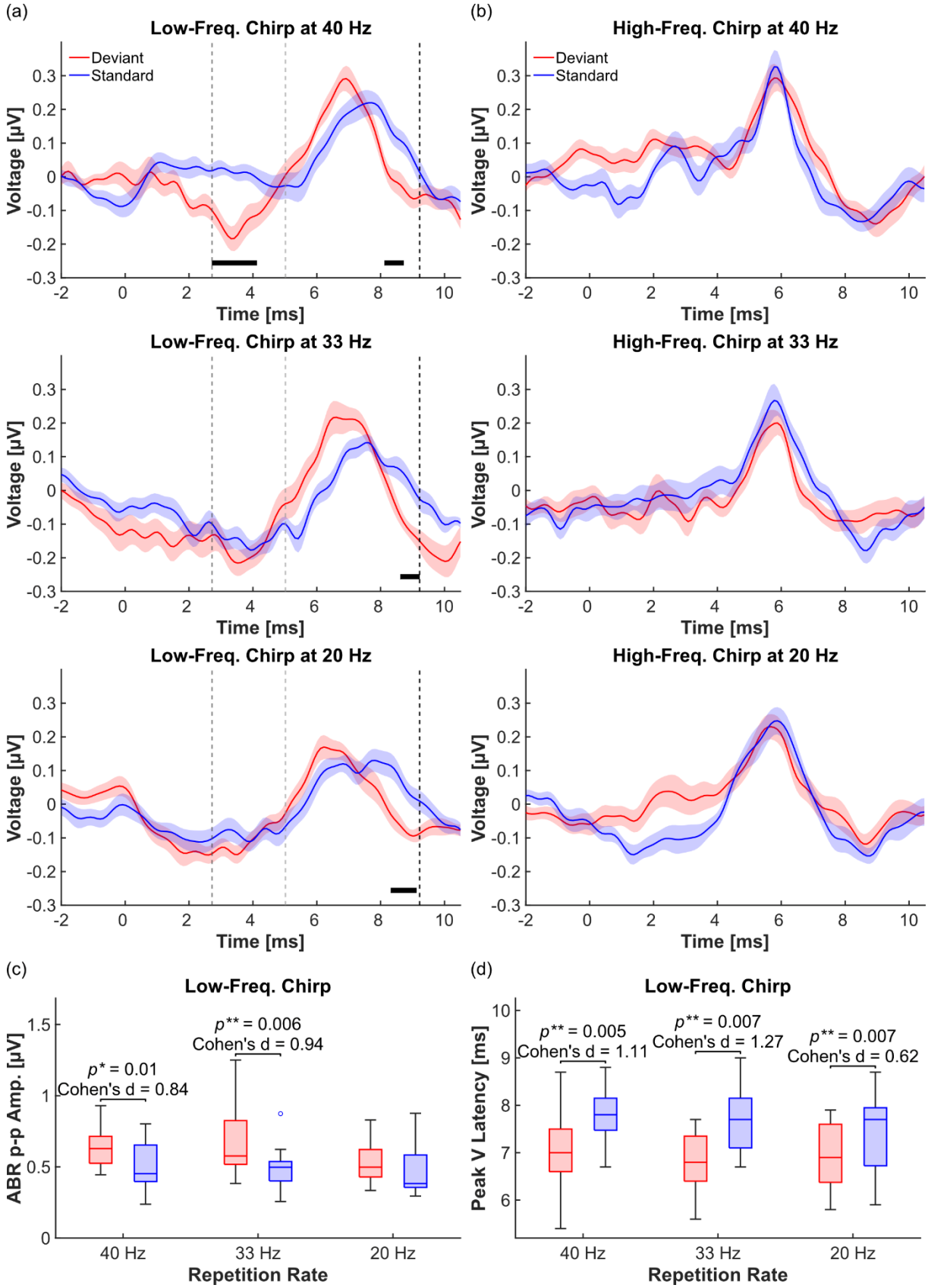


*Figure 2: Deviance detection modulates ABR amplitude and latency (n = 17 subjects). (a) Grand average ABRs elicited by a low-frequency chirp, presented as deviant (red) and standard (blue) at three different stimulus presentation rates (40 Hz, top; 33 Hz, middle; 20 Hz, bottom). The black bars below the ABRs indicate significant differences between deviant and standard waveforms, identified through a cluster-based permutation analysis. Vertical dashed lines mark the time windows used for subsequent amplitude and latency analyses: from the dark grey (first) line to the black (third) line for amplitude analysis and*

*from the light grey (second) line to the black (third) line for peak latency analysis. Shaded areas represent the standard error of the mean. (b) As in (a), but the stimulus was a high-frequency chirp. The cluster-based permutation analysis revealed no significant differences between deviant and standard responses. (c) Boxplots representing the peak-to-peak values of low-frequency chirp ABRs, where red boxes represent deviant responses, and blue boxes represent standard responses. Peak-to-peak values are compared within each stimulus repetition rate. (d) As in (c), but boxplots represent ABR peak V latency.*

**ABR deviance detection is rapid and differentially affects response parameters**

Animal studies have consistently demonstrated that subcortical deviance detection is characterised by a rapid decline in neural responsiveness when the same stimulus is presented repeatedly (Malmierca et al., 2009; Antunes et al., 2010; Bäuerle et al., 2011; Ayala and Malmierca, 2012). To investigate whether the same phenomenon can be observed in humans, we reanalysed the low-frequency chirp data obtained in the oddball paradigm to examine how the standard response develops as the number of repetitions increases (Fig. 3a).

Specifically, we compared the deviant response to the first three standard responses following a deviant. ABR peak-to-peak amplitude and peak V latency were calculated within the same time windows as in the first section of the study (Fig. 3b-d). A two-way ANOVA with the factors of stimulus role (deviant, standard 1, standard 2, standard 3) and repetition rate (40 Hz, 33 Hz, 20 Hz) revealed a significant effect of stimulus role on both ABR peak-to-peak amplitude ($p = 0.036$) and peak V latency ($p = 5.7*10^{-4}$). Subsequent post-hoc t-tests compared the deviant response with each of the standard responses within the same repetition rate. For the 40 Hz rate, a significant difference with a large effect size was found between the deviant and the third standard repetition ($p = 0.026$), indicating a significant repetition suppression effect after no more than three standard repetitions (Fig. 4a, left). Conversely, while a visual inspection suggests a decline in response amplitude at the 33 Hz rate (Fig. 3c), the effect was not statistically significant (Fig. 4a, middle). This indicates that the significant amplitude difference observed at this stimulus presentation rate in the first part of the study (Fig. 2c) only emerges after more than three standard repetitions. Finally, no significant effect was observed for the 20 Hz repetition rate (Fig. 3d; Fig. 4a, right).

Post hoc analysis of ABR peak V latency revealed significant differences between the deviant response and the second ($p = 0.026$, medium effect size) and even the first ($p = 0.021$, large effect size) standard repetition for the 40 Hz and 33 Hz stimulation rates, respectively (Fig.

4b, left and middle). This rapid effect may be attributed to a deviant-related reduction in response latency, either instead of, or in addition to, a standard-related repetition effect at these faster stimulation rates. Regardless of the underlying mechanism, this finding suggests that deviance detection differentially modulates ABR amplitude and latency in humans. For the 20 Hz stimulus presentation rate, the post hoc analysis did not reveal significant differences between the deviant and any of the standard responses (Fig 4b, right), indicating that the latency shift observed at this stimulus presentation rate in the first part of the study (Fig. 2d) requires more than three standard repetitions to emerge.

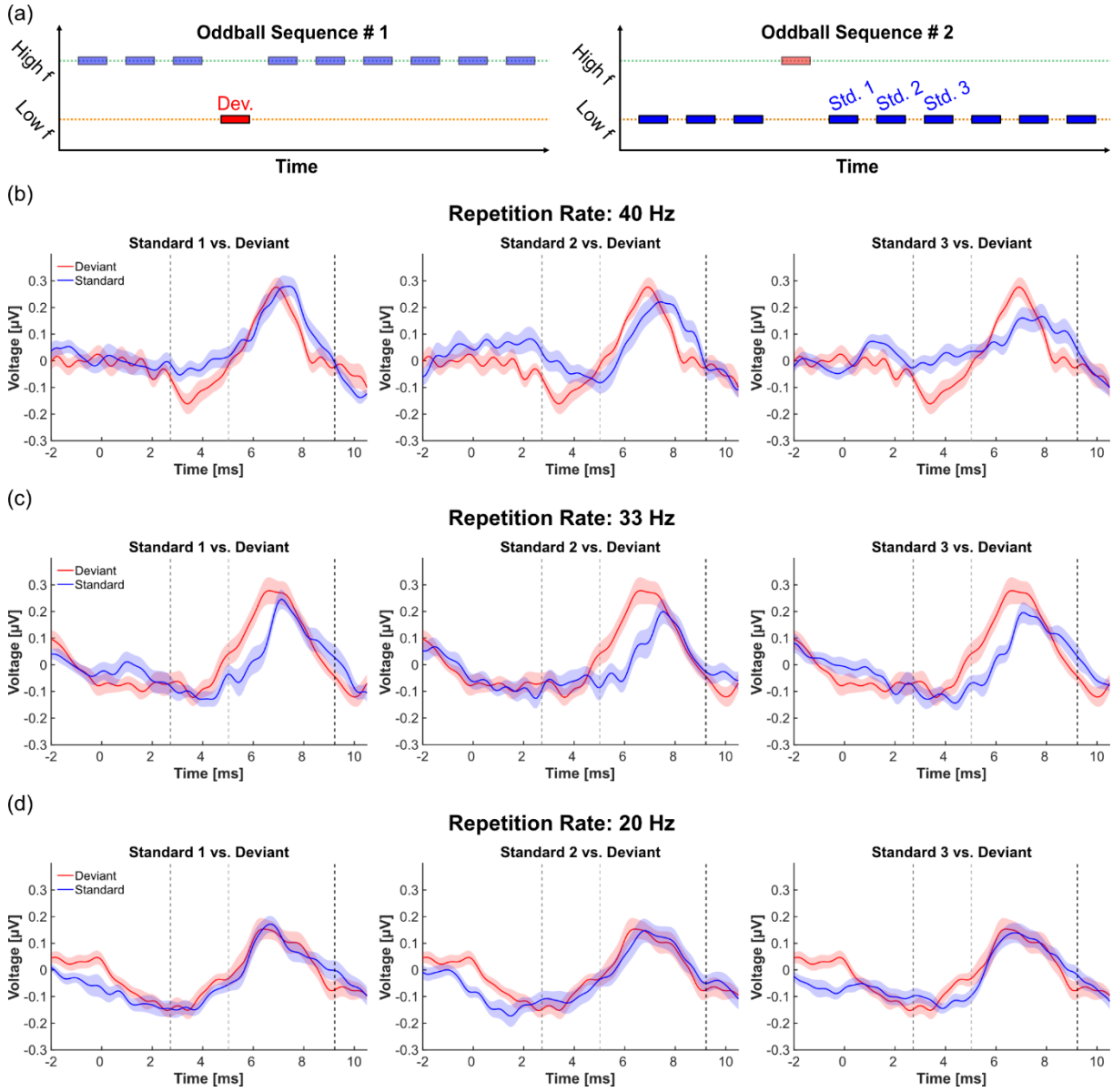


*Figure 3: ABR waveform changes with increasing standard repetition (n = 17 subjects). (a) Schematic representation of the responses illustrated in this figure. Focusing on the low-frequency chirp ABRs, the first three standard responses following a deviant (Std. 1 - Std. 3, blue) are individually compared to the deviant ABRs of the same low-frequency chirp stimulus (Dev., red). (b) Comparison between the deviant ABR and the responses to standards 1-3, presented at a stimulus repetition rate of 40 Hz. Vertical dashed lines indicate the time windows used for subsequent amplitude and latency analyses: from the dark grey (first) line to the black (third) line for amplitude analysis, and from the light grey (second) line to the black (third) line for peak latency analysis (Fig. 4). Shaded areas represent the standard error of the mean. (c) As in (b), but with a stimulus repetition rate of 33 Hz. (d) As in (b), but with a stimulus repetition rate of 20 Hz.*

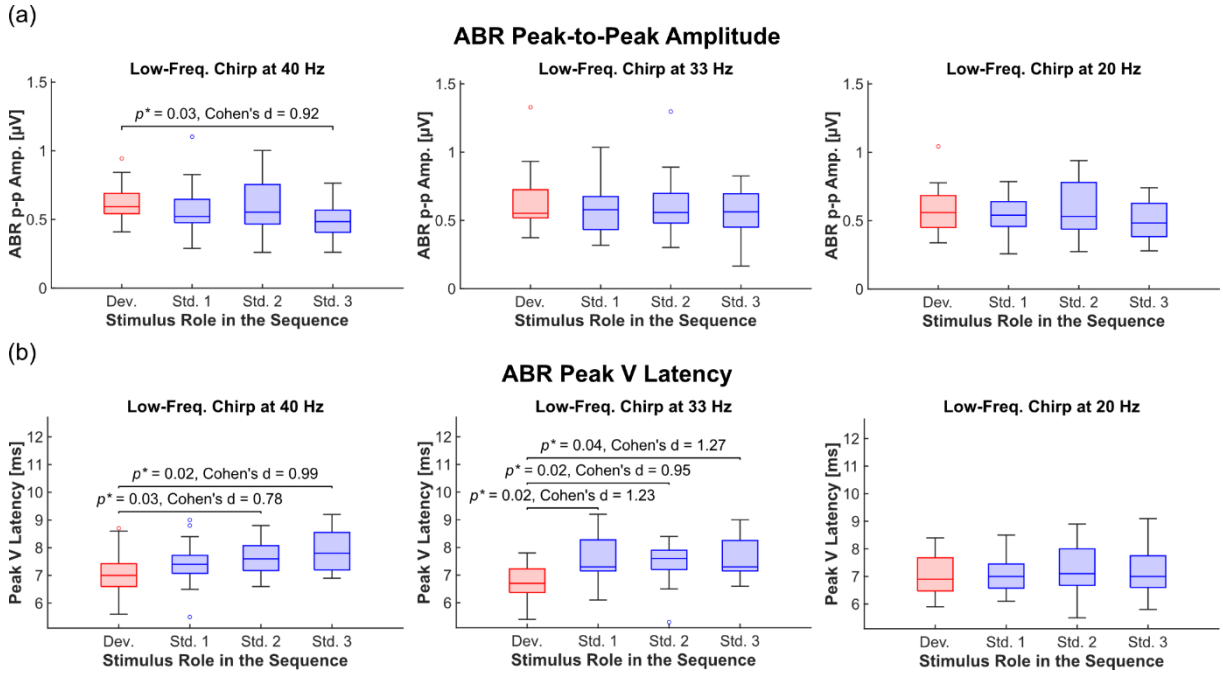


*Figure 4: ABR deviance detection is rapid and differentially affects response parameters (n = 17 subjects). (a) Boxplots showing the peak-to-peak amplitude of ABRs in response to the low-frequency chirp. The peak-to-peak values for the deviant response (red) are compared to those of the first three standard responses following a deviant (blue). The experiment was conducted at three different stimulus repetition rates: 40 Hz (left), 33 Hz (middle), and 20 Hz (right). The data corresponds to the responses illustrated in Fig. 3. (b) As in (a), but the boxplots represent ABR peak V latency.*

## 4. Discussion

This study used ABRs to investigate subcortical auditory deviance detection in humans. When low-frequency chirps were presented as deviants, they elicited significantly larger and faster ABRs compared to when the same stimulus was used as a standard. A trial-by-trial analysis revealed that these differences emerged within up to three repetitions of the standard response at the fastest stimulus presentation rate. Additionally, the findings suggest that subcortical deviance detection is stimulus-specific, as no significant differences were observed between deviant and standard responses for high-frequency chirps.

ABRs are population responses that reflect neural activity across several peripheral auditory nuclei, with the primary generators typically identified as the auditory nerve, cochlear nucleus, superior olivary complex, lateral lemniscus, and IC (Buchwald and Huang, 1975; Henry, 1979; Picton, 2010). Synchronised neural activity within these areas is detected as peaks in the ABR waveform. However, due to the chirp stimuli used, the ABRs recorded in this study were dominated by a large wave V, primarily representing IC activity (Buchwald and Huang, 1975; Henry, 1979; Caird and Klinke, 1987; Land et al., 2016), with earlier waves being less prominent or absent. Consequently, we consider the IC as the main generator of the effects reported here.

To interpret the current findings, it is essential to evaluate them in the context of previous research. The key observations of this study are as follows:

1. Significant deviance detection effects on the ABR waveform are measurable within less than 10 ms after basilar membrane activation.
2. Subcortical deviance detection affects both response amplitude and latency.
3. The influence of deviance detection on these response parameters is both rapid and differential.

4. The effects vary based on stimulus frequency and presentation rate.

These findings are consistent with animal research that has investigated stimulus-specific adaptation (SSA) at the single-unit level in the IC of rats, where deviant stimuli were shown to elicit not only more frequent but also earlier single-neuron responses compared to standard stimuli (Malmierca et al., 2009; Zhao et al., 2011). Moreover, studies in rodents have demonstrated that subcortical SSA occurs within less than ten standard repetitions (Malmierca et al., 2009; Antunes et al., 2010; Bäuerle et al., 2011; Ayala and Malmierca, 2012) and is dependent on the stimulus presentation rate (Malmierca et al., 2009; Antunes et al., 2010; Zhao et al., 2011).

The current study demonstrates that multiple observations previously identified exclusively in animal research also apply to human subcortical deviance detection. Notably, it bridges a longstanding gap between animal and human studies concerning the latency of early deviance detection. While animal studies have shown SSA in the IC with latencies of less than 15 ms (Pérez-González et al., 2005; Malmierca et al., 2009), the earliest deviance detection in humans was so far measured at latencies around 25 to 30 ms after stimulus onset (Slabu et al., 2010; Althen et al., 2011; Grimm and Escera, 2012; Shiga et al., 2015). Our ABR data now show that deviance detection with latencies below 10 ms also occurs in humans, suggesting similar temporal dynamics in subcortical deviance detection processing across species.

Deviance detection is often discussed within the framework of predictive coding, a proposed mechanism of the brain to efficiently manage the vast amount of sensory input it receives. The theory suggests that the brain continuously predicts near-future events and compares these internal predictions with actual sensory input. When there is a mismatch between input and expectation, a prediction error is generated, which is then used to update the predictive model (Friston, 2005; Winkler, 2007). Detecting unexpected events, therefore, plays a crucial role in the predictive coding framework, and evidence supporting this mechanism of sensory

processing has been steadily accumulating (Winkler, 2007; Auksztulewicz and Friston, 2016; Parras et al., 2017; Carbajal and Malmierca, 2018; Fitzgerald and Todd, 2020; Quintela-Vega et al., 2023; Song et al., 2023; Tzovara et al., 2024). A widely discussed concept is that the auditory system is hierarchically organised, with higher-order brain regions generating predictions that are projected top-down, while lower-order regions generate prediction errors that are sent bottom-up to update predictions in higher centres (Grimm and Escera, 2012; Escera and Malmierca, 2014; Tabas and von Kriegstein, 2021; Escera, 2023). Supporting this hierarchical model, research has shown that the complexity of novelty detection increases with each station along the ascending auditory pathway (Parras et al., 2017; Carbajal and Malmierca, 2018; Escera, 2023). The subcortical deviance detection effects reported here, which are based on simple carrier frequency deviants, align well with this established model of a hierarchically organised regularity-encoding system. However, a critical element of the predictive coding framework is the prediction error component, which can be assessed through specific control experiments like the many-standards paradigm (Schröger and Wolff, 1996) or the cascade control (Ruhnau et al., 2012). Since these controls were not included in this study, we were unable to investigate the prediction error component, and future research should aim to explore this aspect further.

The finding that significant deviance detection emerges after only a few standard repetitions is consistent with previous research in animals (Malmierca et al., 2009; Antunes et al., 2010; Bäuerle et al., 2011; Ayala and Malmierca, 2012). However, to our knowledge, this study presents the first evidence of an differential influence of deviance detection on subcortical response amplitude and latency. While amplitude differences between deviant and standard responses only become evident after three or more standard repetitions, latency differences can be observed as early as the first standard repetition at certain stimulus presentation rates. One possible explanation for this phenomenon is that the shorter latency observed for deviant

responses, compared to standard responses, may not be solely attributable to an increasing delay of the standard response with each repetition (repetition delay). Instead, it could involve an additional reduction in response latency when a deviant is detected. This could be interpreted as a prediction error component operating within the time domain. Nevertheless, as mentioned earlier, further control recordings would be necessary to validate this hypothesis and to confirm the existence of a prediction error component.

Another open question that arises is why significant deviance detection was only elicited by the low-frequency chirp. Similar findings have been observed in bat ABRs (Wetekam et al., 2024) and human FFRs (Slabu et al., 2012), but the underlying reasons remain unclear. In our study, one possible explanation for this discrepancy may stem from research on repetition suppression. These studies have shown that repetition suppression, a key mechanism in deviance detection, is more commonly observed for familiar sounds compared to unfamiliar ones (Henson et al., 2000; Müller et al., 2013; Segaert et al., 2013). The spectrum of our low-frequency chirp (500-2000 Hz) comprises most of the frequencies typically encountered in daily life, making it a potentially more familiar stimulus compared to the high-frequency chirp (2000-8000 Hz). Furthermore, high-pitched sounds are often associated with alarm signals (Zeskind and Collins, 1987; Haas and Edworthy, 1996; Schwartz and Gouzoules, 2019), which may gain behavioural relevance when perceived repeatedly. Consequently, the primary goal of processing high-frequency stimuli might not be to maximise efficiency, but rather to maintain an effective alarm signal that does not diminish with repeated exposure. These hypotheses should be addressed in future research, together with a more detailed investigation of the specific stimulus parameters required to elicit mismatch responses in ABRs, e.g. identifying the frequency threshold below which deviance detection becomes measurable.

Beyond stimulus frequency, other parameters of stimulation, such as the stimulus repetition rate, have also been shown to significantly influence subcortical deviance detection in animals (Malmierca et al., 2009; Antunes et al., 2010; Zhao et al., 2011). While our data corroborate this dependency, it is important to note that the stimulus repetition rates employed in the present study (40 Hz, 33 Hz, and 20 Hz) were faster than those used in previous research on subcortical deviance detection in humans (Slabu et al., 2012: 3.3 Hz; Cacciaglia et al., 2015: 6.6 Hz; Tabas et al., 2020: 1.4 Hz). The current results suggest that mismatch responses in ABRs decrease with the stimulus presentation rate, making it unlikely that significant effects would have been observed at repetition rates below 10 Hz. This may also explain why two earlier studies failed to detect an effect of stimulus probability on ABRs (Slabu et al., 2010; Althen et al., 2011). In those studies, the authors used lower stimulus repetition rates of approximately 10 Hz (Slabu et al., 2010) and 3 Hz (Althen et al., 2011), along with higher deviant probabilities of 1/5 (Slabu et al., 2010) and 1/7 (Althen et al., 2011). Collectively, these findings indicate that ABR-based mismatch responses are elicited at higher repetition rates than those deviance detection effects seen in fMRI or FFR data. This suggests that both phenomena operate on different time scales and highlights the importance of optimising stimulation parameters in dependence of the methodological approach.

## Conclusion

This study revealed that subcortical auditory deviance detection in humans is both rapid and stimulus-specific, with significant modulation of ABR amplitude and latency occurring within just a few stimulus repetitions. The identification of mismatch responses at latencies below 10 ms helps to bridge the gap between human and animal research, indicating similar temporal dynamics across species. Moreover, the study highlights the value of ABR recordings for investigating subcortical auditory deviance detection, due to its excellent temporal resolution in comparison to other non-invasive methods.

## Author contributions

Study design: Johannes Wetekam, Nell Gotta, Luciana López-Jury, Julio Hechavarría, Manfred Kössl

Experiments: Johannes Wetekam, Nell Gotta

Analysis, and original draft of the manuscript: Johannes Wetekam

Review and editing of the original draft: Johannes Wetekam, Nell Gotta, Luciana López-Jury, Julio Hechavarría, Manfred Kössl

## Abbreviations

| | |
|---|---|
| ABR: | Auditory brainstem response |
| EEG: | Electroencephalography |
| FFR: | Frequency-following response |
| fMRI: | Functional magnetic resonance imaging |
| IC: | Inferior colliculus |
| MEG: | Magnetoencephalography |
| MMN: | Mismatch negativity |
| SSA: | Stimulus-specific adaptation |

# References


Althen H, Grimm S, Escera C (2011) Fast detection of unexpected sound intensity decrements as revealed by human evoked potentials. PLoS ONE 6.

Antunes FM, Nelken I, Covey E, Malmierca MS (2010) Stimulus-specific adaptation in the auditory thalamus of the anesthetized rat. PLoS ONE 5.

Auksztulewicz R, Friston K (2016) Repetition suppression and its contextual determinants in predictive coding. Cortex 80:125–140.

Ayala YA, Malmierca MS (2012) Stimulus-specific adaptation and deviance detection in the inferior colliculus. Frontiers in Neural Circuits 6:1–16.

Bäuerle P, von der Behrens W, Kössl M, Gaese BH (2011) Stimulus-specific adaptation in the gerbil primary auditory thalamus is the result of a fast frequency-specific habituation and is regulated by the corticofugal system. Journal of Neuroscience 31:9708–9722.

Benjamini Y, Hochberg Y (1995) Controlling the False Discovery Rate: A Practical and Powerful Approach to Multiple Testing. Journal of the Royal Statistical Society: Series B (Methodological) 57:289–300.

Buchwald JS, Huang C-M (1975) Far-Field Acoustic Response: Origins in the Cat. Science 189:382–384.

Cacciaglia R, Escera C, Slabu L, Grimm S, Sanjuán A, Ventura-Campos N, Ávila C (2015) Involvement of the human midbrain and thalamus in auditory deviance detection. Neuropsychologia 68:51–58.

Caird DM, Klinke R (1987) The effect of inferior colliculus lesions on auditory evoked potentials. Electroencephalogr Clin Neurophysiol 68:237–240.

Candia-Rivera D, Valenza G (2022) Cluster permutation analysis for EEG series based on non-parametric Wilcoxon–Mann–Whitney statistical tests. SoftwareX 19:101170.

Carbajal GV, Malmierca MS (2018) The Neuronal Basis of Predictive Coding Along the Auditory Pathway: From the Subcortical Roots to Cortical Deviance Detection. Trends in Hearing 22:1–33.

Chandrasekaran B, Hornickel J, Skoe E, Nicol T, Kraus N (2009) Context-Dependent Encoding in the Human Auditory Brainstem Relates to Hearing Speech in Noise: Implications for Developmental Dyslexia. Neuron 64:311–319.

Coffey EBJ, Herholz SC, Chepesiuk AMP, Baillet S, Zatorre RJ (2016) Cortical contributions to the auditory frequency-following response revealed by MEG. Nature Communications 7.

Coffey EBJ, Nicol T, White-Schwoch T, Chandrasekaran B, Krizman J, Skoe E, Zatorre RJ, Kraus N (2019) Evolving perspectives on the sources of the frequency-following response. Nature Communications 10:1–10.

Cohen J (1988) Statistical Power Analysis for the Behavioral Sciences. New York.

Don M, Kwong B, Tanaka C (2005) A diagnostic test for Ménière's disease and cochlear hydrops: Impaired high-pass noise masking of auditory brainstem responses. Otology and Neurotology 26:711–722.

Duque D, Pais R, Malmierca MS (2018) Stimulus-specific adaptation in the anesthetized mouse revealed by brainstem auditory evoked potentials. Hearing Research 370:294–301.

Elberling C, Don M (2008) Auditory brainstem responses to a chirp stimulus designed from derived-band latencies in normal-hearing subjects. The Journal of the Acoustical Society of America 124:3022–3037.

Elberling C, Don M, Cebulla M, Stürzebecher E (2007) Auditory steady-state responses to chirp stimuli based on cochlear traveling wave delay. The Journal of the Acoustical Society of America 122:2772.

Escera C (2023) Contributions of the subcortical auditory system to predictive coding and the neural encoding of speech. Current Opinion in Behavioral Sciences 54:101324.

Escera C, Leung S, Grimm S (2014) Deviance detection based on regularity encoding along the auditory hierarchy: Electrophysiological evidence in humans. Brain Topography 27:527–538.

Escera C, Malmierca MS (2014) The auditory novelty system: An attempt to integrate human and animal research. Psychophysiology 51:111–123.

Fitzgerald K, Todd J (2020) Making Sense of Mismatch Negativity. Frontiers in Psychiatry 11:468.

Fobel O, Dau T (2004) Searching for the optimal stimulus eliciting auditory brainstem responses in humans. The Journal of the Acoustical Society of America 116:2213–2222.

Friston K (2005) A theory of cortical responses. Philosophical Transactions of the Royal Society B: Biological Sciences 360:815–836.

Grimm S, Escera C (2012) Auditory deviance detection revisited: Evidence for a hierarchical novelty system. International Journal of Psychophysiology 85:88–92.

Haas EC, Edworthy J (1996) Designing urgency into auditory warnings using pitch, speed and loudness. Computing & Control Engineering Journal 7:193–198.

Henry KR (1979) Auditory brainstem volume-conducted responses: Origins in the laboratory mouse. Journal of the American Auditory Society 4:173–178.

Henson R, Shallice T, Dolan R (2000) Neuroimaging Evidence for Dissociable Forms of Repetition Priming. Science 287:1269–1272.

Kraus N, McGee T, Carrell T, King C, Littman T, Nicol T (1994a) Discrimination of speech-like contrasts in the auditory thalamus and cortex. The Journal of the Acoustical Society of America 96:2758–2768.

Kraus N, McGee T, Littman T, Nicol T, King C (1994b) Nonprimary auditory thalamic representation of acoustic change. Journal of Neurophysiology 72:1270–1277.

Land R, Burghard A, Kral A (2016) The contribution of inferior colliculus activity to the auditory brainstem response (ABR) in mice. Hearing Research 341:109–118.

Malmierca MS, Cristaudo S, Pérez-González D, Covey E (2009) Stimulus-specific adaptation in the inferior colliculus of the anesthetized rat. Journal of Neuroscience 29:5483–5493.

Müller NG, Strumpf H, Scholz M, Baier B, Melloni L (2013) Repetition Suppression versus Enhancement—It's Quantity That Matters. Cerebral Cortex 23:315–322.

Näätänen R, Gaillard AWK, Mäntysalo S (1978) Early selective-attention effect on evoked potential reinterpreted. Acta Psychologica 42:313–329.

Näätänen R, Paavilainen P, Rinne T, Alho K (2007) The mismatch negativity (MMN) in basic research of central auditory processing: A review. Clinical Neurophysiology 118:2544–2590.

Nelken I (2014) Stimulus-specific adaptation and deviance detection in the auditory system: experiments and models. Biological Cybernetics 108:655–663.

Parras GG, Nieto-Diego J, Carbajal GV, Valdés-Baizabal C, Escera C, Malmierca MS (2017) Neurons along the auditory pathway exhibit a hierarchical organization of prediction error. Nature Communications 8.

Patel CR, Redhead C, Cervi AL, Zhang H (2012) Neural sensitivity to novel sounds in the rat's dorsal cortex of the inferior colliculus as revealed by evoked local field potentials. Hearing Research 286:41–54.

Pérez-González D, Malmierca MS, Covey E (2005) Novelty detector neurons in the mammalian auditory midbrain. European Journal of Neuroscience 22:2879–2885.

Picton TW (2010) Auditory brainstem responses: peaks along the way. Human auditory evoked potentials:213–246.

Quintela-Vega L, Morado-Díaz CJ, Terreros G, Sánchez JS, Pérez-González D, Malmierca MS (2023) Novelty detection in an auditory oddball task on freely moving rats. Commun Biol 6:1–15.

Ruhnau P, Herrmann B, Schröger E (2012) Finding the right control: The mismatch negativity under investigation. Clinical Neurophysiology 123:507–512.

Schröger E, Wolff C (1996) Mismatch response of the human brain to changes in sound location. NeuroReport 7:3005–3008.

Schwartz JW, Gouzoules H (2019) Decoding human screams: perception of emotional arousal from pitch and duration. Behaviour 156:1283–1307.

Segaert K, Weber K, de Lange FP, Petersson KM, Hagoort P (2013) The suppression of repetition enhancement: A review of fMRI studies. Neuropsychologia 51:59–66.

Shiga T, Althen H, Cornella M, Zarnowiec K, Yabe H, Escera C (2015) Deviance-related responses along the auditory hierarchy: Combined FFR, MLR and MMN evidence. PLoS ONE 10:1–14.

Skoe E, Kraus N (2010) Hearing It Again and Again: On-Line Subcortical Plasticity in Humans. PLOS ONE 5:e13645.

Slabu L, Escera C, Grimm S, Costa-Faidella J (2010) Early change detection in humans as revealed by auditory brainstem and middle-latency evoked potentials. European Journal of Neuroscience 32:859–865.

Slabu L, Grimm S, Escera C (2012) Novelty Detection in the human auditory brainstem. Journal of Neuroscience 32:1447–1452.

Song P, Zhai Y, Yu X (2023) Stimulus-specific adaptation (SSA) in the auditory system: Functional relevance and underlying mechanisms. Neuroscience & Biobehavioral Reviews 149:105190.

Tabas A, Kriegstein K von (2024) Multiple Concurrent Predictions Inform Prediction Error in the Human Auditory Pathway. J Neurosci 44 Available at: https://www.jneurosci.org/content/44/1/e2219222023 [Accessed June 12, 2024].

Tabas A, Mihai G, Kiebel S, Trampel R, von Kriegstein K (2020) Abstract rules drive adaptation in the subcortical sensory pathway Shinn-Cunningham BG, Griffiths TD, Malmierca MS, eds. eLife 9:e64501.

Tabas A, von Kriegstein K (2021) Adjudicating Between Local and Global Architectures of Predictive Processing in the Subcortical Auditory Pathway. Front Neural Circuits 15:644743.

Tzovara A, Fedele T, Sarnthein J, Ledergerber D, Lin JJ, Knight RT (2024) Predictable and unpredictable deviance detection in the human hippocampus and amygdala. Cerebral Cortex:bhad532.

Ulanovsky N, Las L, Farkas D, Nelken I (2004) Multiple time scales of adaptation in auditory cortex neurons. Journal of Neuroscience 24:10440–10453.

Ulanovsky N, Las L, Nelken I (2003) Processing of low-probability sounds by cortical neurons. Nature Neuroscience 6:391–398.

Wetekam J, Hechavarría J, López-Jury L, González-Palomares E, Kössl M (2024) Deviance detection to natural stimuli in population responses of the brainstem of bats. J Neurosci:e1588232023.

Wetekam J, Hechavarría J, López-Jury L, Kössl M (2022) Correlates of deviance detection in auditory brainstem responses of bats. European Journal of Neuroscience 55:1601–1613.

Winkler I (2007) Interpreting the mismatch negativity (MMN). Journal of Psychophysiology - J PSYCHOPHYSIOL 21:147–163.

Zeskind PS, Collins V (1987) Pitch of infant crying and caregiver responses in a natural setting. Infant Behavior and Development 10:501–504.

Zhao L, Liu Y, Shen L, Feng L, Hong B (2011) Stimulus-specific adaptation and its dynamics in the inferior colliculus of rat. Neuroscience 181:163–174.

## Figure legends

Figure 1: Used stimuli and stimulation protocol. (a) Spectrograms (top) and oscillograms (bottom) of a low-frequency chirp (orange frame) and a high-frequency chirp (green frame) that were used as stimuli in this study. (b) Schematic representation of the oddball paradigm; blue: high-probability standard, red: low-probability deviant.

Figure 2: Deviance detection modulates ABR amplitude and latency (n = 17 subjects). (a) Grand average ABRs elicited by a low-frequency chirp, presented as deviant (red) and standard (blue) at three different stimulus presentation rates (40 Hz, top; 33 Hz, middle; 20 Hz, bottom). The black bars below the ABRs indicate significant differences between deviant and standard waveforms, identified through a cluster-based permutation analysis. Vertical dashed lines mark the time windows used for subsequent amplitude and latency analyses: from the dark grey (first) line to the black (third) line for amplitude analysis and from the light grey (second) line to the black (third) line for peak latency analysis. Shaded areas represent the standard error of the mean. (b) As in (a), but the stimulus was a high-frequency chirp. The cluster-based permutation analysis revealed no significant differences between deviant and standard responses. (c) Boxplots representing the peak-to-peak values of low-frequency chirp ABRs, where red boxes represent deviant responses, and blue boxes represent standard responses. Peak-to-peak values are compared within each stimulus repetition rate. (d) As in (c), but boxplots represent ABR peak V latency.

Figure 3: ABR waveform changes with increasing standard repetition (n = 17 subjects). (a) Schematic representation of the responses illustrated in this figure. Focusing on the low-frequency chirp ABRs, the first three standard responses following a deviant (Std. 1 - Std. 3, blue) are individually compared to the deviant ABRs of the same low-frequency chirp stimulus (Dev., red). (b) Comparison between the deviant ABR and the responses to standards 1-3, presented at a stimulus repetition rate of 40 Hz. Vertical dashed lines indicate the time

windows used for subsequent amplitude and latency analyses: from the dark grey (first) line to the black (third) line for amplitude analysis, and from the light grey (second) line to the black (third) line for peak latency analysis (Fig. 4). Shaded areas represent the standard error of the mean. (c) As in (b), but with a stimulus repetition rate of 33 Hz. (d) As in (b), but with a stimulus repetition rate of 20 Hz.

Figure 4: ABR deviance detection is rapid and differentially affects response parameters (n = 17 subjects). (a) Boxplots showing the peak-to-peak amplitude of ABRs in response to the low-frequency chirp. The peak-to-peak values for the deviant response (red) are compared to those of the first three standard responses following a deviant (blue). The experiment was conducted at three different stimulus repetition rates: 40 Hz (left), 33 Hz (middle), and 20 Hz (right). The data corresponds to the responses illustrated in Fig. 3. (b) As in (a), but the boxplots represent ABR peak V latency.